ORGANIC CHEMISTRY FRONTIERS

RESEARCH ARTICLE

View Article Online
View Journal | View Issue

Cite this: *Org. Chem. Front.*, 2025, **12**, 5783

Benzylic C–H bond functionalization through photo-mediated mesyloxy radical formation†

Jannik Thaens, ‡ Xinzhe Shi, ‡§ Tobias Taeufer, Janina Schlapp and Jola Pospech *

Received 24th April 2025,
Accepted 30th June 2025

DOI: 10.1039/d5qo00683j

rsc.li/frontiers-organic

Herein, we report a photo-mediated methodology for benzylic C–H bond oxygenation. Our approach employs *in situ* generated (methylsulfonyloxy)pyridinium mesylate salts to produce mesyloxy radicals apt for benzylic C–H bond cleavage through hydrogen atom transfer (HAT). Subsequent oxidation of the benzylic radical yields a carbocation, functionalized by the mesylate counterion through oxidative radical-polar crossover (ORPC). The reactive benzylic mesylates are converted into stable benzylic alcohols *via* a straightforward protocol. Reaction optimization utilized modern design of experiment (DoE) techniques for facile setups and rapid reactions. Our proposed mechanistic paradigm is supported by comprehensive investigations, including fluorescence quenching studies, cyclic voltammetry measurements, and determination of kinetic isotope effects (KIEs). Density functional theory (DFT) calculations elucidate the divergent performance of (methylsulfonyloxy)pyridinium salts and (trifluoromethylsulfonyloxy)pyridinium salts.

The functionalization of unactivated C–H bonds represents a versatile strategy for the diversification of drug intermediates in synthetic organic chemistry.[1,2] Besides transition metal catalysis, electrosynthesis or biocatalysis, the utilization of radical species for C–H bond functionalization has been rapidly gaining attention.[3–8] In the past, radicals were frequently generated under harsh reaction conditions, restricting compatibility with functional groups. However, the advent of photoredox catalysis has facilitated the generation of radicals under mild conditions.[9,10] In this context, redox-active pyridinium salts have served as unique radical precursors, generating reactive species after single-electron reduction by an appropriate photoredox catalyst.[11–15] Electronic effects have a significant impact on the generation and reactivity of radical species.[16] For instance, the electronic properties of both the exocyclic and heteroarene substituents in redox-active pyridinium salts play a crucial role in dictating the formation of N-centered *versus* X-centered radicals through dissociative electron transfer (DET) (Fig. 1).[17] Strongly electron withdrawing *N*-substituents **X** (*e.g.* TfO^- and F^-) favour heterolytic bond cleavage generating N-centered pyridinium radicals $\mathbf{py}^{\bullet+}$ and less electron-withdrawing *N*-substituents (*e.g.* F_3CO^- and RO^-) favour homolytic bond-cleavage generating an X-centered radical $\mathbf{X}^{\bullet}$. It has been demonstrated that the resulting radicals can undergo a variety of chemical transformations, which were applied in both $C(sp^2)$–H and $C(sp^3)$–H bond functionalisations.[18]

The photo-mediated amination of aromatic $C(sp^2)$–H bonds by means of the heterolytic bond breaking of redox-active pyridinium salts was described by Studer,[19] Ritter[20] and Carreira[21] (Scheme 1, top left). In contrast, the more common homolysis of *N*-functionalized pyridinium salt N–X bonds enables the formation of a plethora of radical species depending on the *N*-substituent.[17] Oxygen-, nitrogen-, and carbon-centered rad-

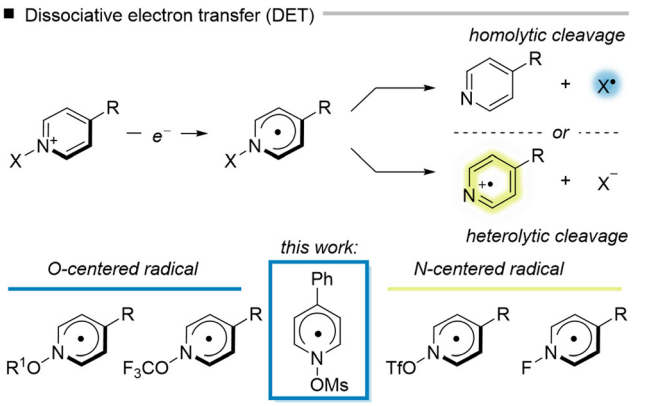

Fig. 1 Homolytic and heterolytic bond cleavage of redox-active pyridinium salts.

Leibniz Institute for Catalysis, Albert-Einstein-Str. 29a, 18059 Rostock, Germany. E-mail: Jola.Pospech@catalysis.de

†Electronic supplementary information (ESI) available. CCDC 2345289 and 2348388. For ESI and crystallographic data in CIF or other electronic format see DOI: https://doi.org/10.1039/d5qo00683j

‡These authors contributed equally.

§School of Chemistry and Chemical Engineering, Harbin Institute of Technology, Harbin 150001, P. R. China.

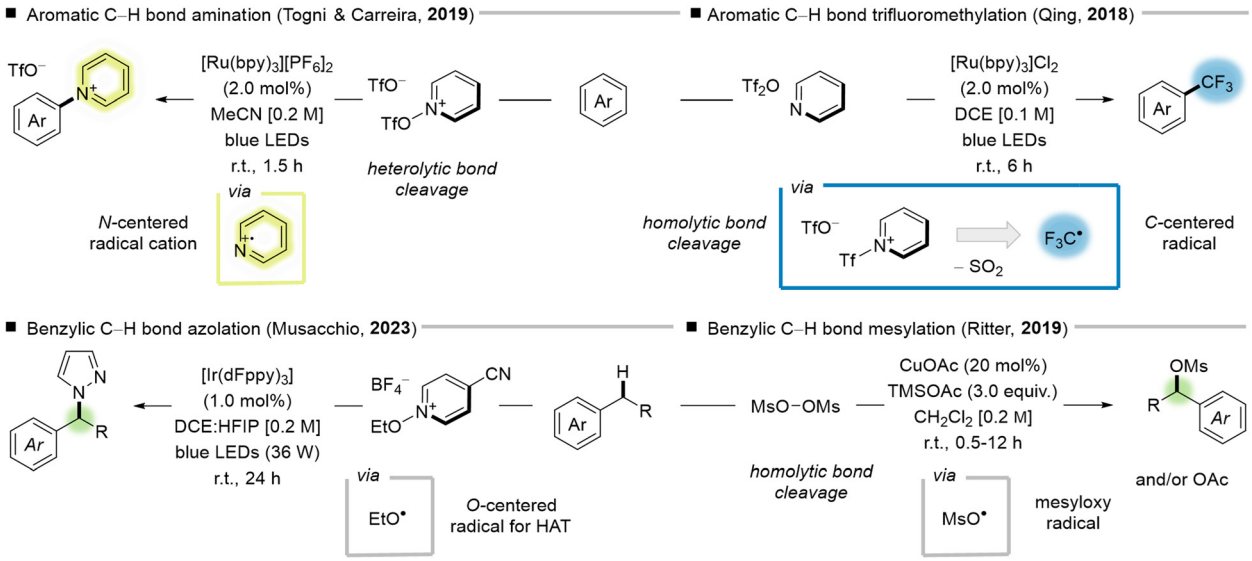

Scheme 1 Selected examples of pyridinium salts as group transfer reagents.

icals have been effectively generated and utilized in direct trifluoromethoxylation,[22] amination,[23,24] and alkylation[25–28] reactions of C(sp^2)–H bonds. Notably, trifluoroacetic anhydride and trifluoromethanesulfonic anhydride, in combination with pyridine *N*-oxides and pyridine, respectively, have been utilized for trifluoromethylation of arenes and functionalization of C–C multiple bonds (Scheme 1, top right).[29–32] To the best of our knowledge, the formation of O-centered triflyloxy radicals is unprecedented. The electron-withdrawing fluorine substituents destabilize the corresponding O-centered radical, resulting in a trifluoromethyl radical $F_3C^{\bullet}$ upon expulsion of CO_2 and SO_2, respectively.[33] In addition to C(sp^2)–H bond derivatization, O-centered radicals have been found to trigger radical hydrogen atom abstraction from C(sp^3)–H bonds, provided that a thermodynamic driving force is apparent (BDE_{C-H} < BDE_{O-H}). This method presents a mild and adaptable technique for cleaving C(sp^3)–H bonds for the generation of carbon-centered radicals that are apt for subsequent reactions.[34,35] For instance, oxidative radical-polar crossover (ORPC) is a process in which a radical undergoes oxidation to form a carbocation. This approach has been identified as a promising strategy for the functionalization of C(sp^3)–H bonds with a wide range of nucleophiles, exhibiting both abundance and structural diversity. ORPC-based methodologies have been developed for the photo-mediated hydroxylation,[36,37] alkoxylation,[38–43] esterification,[44] amination,[45] and fluorination[46,47] of benzylic C–H bonds of electron-rich substrates. Furthermore, the Musacchio group was able to describe benzylic azolation in 2023 (Scheme 1, bottom left).[48] The key intermediate in the form of an ethoxy radical was generated *via* the photochemical reduction of the corresponding pyridinium salt. Along this line, in 2019, Ritter and co-workers published a methodology for the oxygenation of benzylic C–H bonds utilizing electrochemically synthesized methanesulfonic peroxyanhydride as a mesyloxy radical precursor (Scheme 1, bottom right).[49] To date, only two reactions involving mesyloxy radicals have been showcased.[49,50]

Drawing from our interest in heteroarene-*N*-oxide-mediated oxygenation procedures, we set out to investigate the DET of (methylsulfonyloxy)pyridinium salts upon photo-mediated single-electron reduction. We questioned whether (methylsulfonyloxy)pyridinium salts, which lack literature precedence, would (i) undergo heterolytic bond cleavage similar to their trifluoromethylsulfonyloxy-pyridinium salt analogs[21] or (ii) undergo homolytic bond cleavage, generating a methylsulfonyloxy radical that, in contrast to trifluoromethylsulfonyloxy radicals, should be stable as demonstrated by Ritter and co-workers.[49]

1-(Methylsulfonyloxy)pyridinium methanesulfonate (**2**) can be synthesized on a decagram scale from pyridine-*N*-oxide **4ab** and methanesulfonic anhydride.[51] To evaluate the feasibility of a direct benzylic C–H mesyloxylation using (methylsulfonyloxy)pyridinium salts, we investigated the conversion of 1-bromo-4-ethylbenzene (**1a**) into 1-(4-bromophenyl)ethyl methanesulfonate (**3a**) using the pre-formed 1-(methylsulfonyloxy)pyridinium methanesulfonate (**2**) (Scheme 2, top). Pyridinium methanesulfonate **2** exhibits a ground-state reduction potential of $E^{red}_{1/2}$ = −0.42 V in MeCN *vs.* SCE and thus should be readily reduced by $[Ru(bpy)_3][PF_6]_2$ (E^{*}_{ox} = −0.81 V *vs.* SCE in MeCN, λ^{abs}_{max} = 450 nm) as a photoredox catalyst upon irradiation with blue light (3 × 7 W LED, λ^{em}_{max} = 458 nm).[52] To our delight, the desired mesyloxylated product **3a** was formed readily in 59% yield according to ^{1}H-NMR spectroscopy. More importantly, the utilization of equimolar amounts of pyridine *N*-oxide (**4a**) and methanesulfonic anhydride allowed for an *in situ* formation of the pivotal redox-active pyridinium mesylate agent with marginal deterioration in yield (Scheme 2, bottom). In addition, we found that

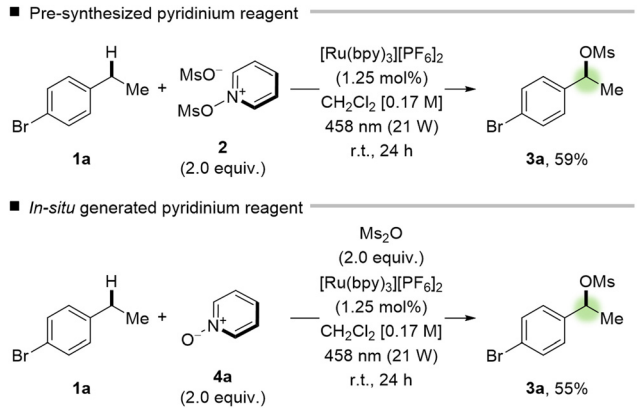

Scheme 2 Benzylic C–H bond mesyloxylation with pre-formed and *in situ* generated (methylsulfonyloxy)pyridinium salts.

reducing the wattage from 21 to 14 W had no detrimental effect on the yield of the desired product **3a**. Notably, benzylic mesylates **3** exhibit thermal instability and undergo elimination to form styrene byproducts at elevated temperatures, including during GC analysis.

The reliable *in situ* formation of the pyridinium salt significantly accelerated the subsequent screening of various heteroarene *N*-oxides **4a–4g** (Table 1). Pyrazine and pyrimidine *N*-oxides (**4b** and **4c**) led to diminished product yields (Table 1, entries 2 and 3). Similarly, substitution with electron-withdrawing and electron-donating substituents **4d**, **4e** and **4f** also resulted in lower product yields compared to pyridine *N*-oxide (Table 1, entries 4–6). The best result was obtained using 4-phenylpyridine *N*-oxide (**4g**) (Table 1, entry 7). Increasing the amounts of *N*-oxide **4g** and methanesulfonic anhydride to 3.0 equiv. led to full conversion of the starting material **1a** along with an increased yield of 70%. Reaction monitoring ^{1}H-NMR analysis of the crude reaction mixture showed that a maximum conversion to the desired product **4g** is already reached after a reaction time of 90 min (Table 1, entry 9). After 16 hours, the product yield of mesylate **3a** is in fact diminished due to the formation of side products (Table 1, entry 8).[53] Consequently, irradiation at 458 nm (14 W) for 1.5 h enabled the formation of the desired product in an NMR yield of 83% (Table 1, entry 9).

The optimization of molar ratios of the reactants was evaluated by conducting a Design of Experiment (DoE) assay.[54] For the DoE, a face-centered design with three variables, focusing on the stoichiometry of the reactants 4-bromoethylbenzene (**1a**), 4-phenylpyridine *N*-oxide (**4g**), and methanesulfonic anhydride, was applied (for more details, see the ESI†). The response surface was calculated using a quadratic model. The graphical analysis of the screening set using the substrate **1a** as the limiting reagent is depicted in Fig. 2. The assay supports the results from the one parameter optimization. The optimal

Table 1 Screening of heteroarene *N*-oxides **4a–4g**[a]

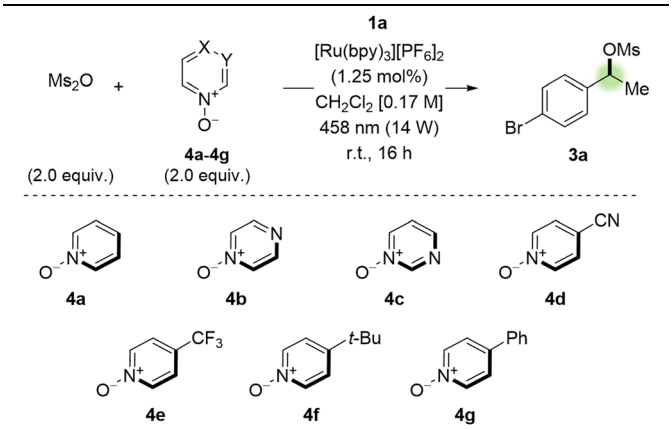

Entry	HetAr *N*-oxide	Equiv. of **4**[b]	Wattage [W]	Conv. of **1a**[c] [%]	Conv. to **3a**[c,d] [%]
1	**4a**	2.0	21	61	55
2	**4b**	2.0	21	<5	<5
3	**4c**	2.0	21	13	10
4	**4d**	2.0	21	18	11
5	**4e**	2.0	21	26	9
6	**4f**	2.0	21	25	20
7	**4g**	2.0	21	88	65
8	**4g**	3.0	21	>95[d]	87[c], 70[d]
9[e]	**4g**	3.0	14	>95[d]	83[d,e]

[a] Reactions were performed on a 0.5 mmol scale. [b] Heteroarene *N*-oxides **4** and Ms_2O were used in a 1 : 1 ratio. [c] Conversions were determined by calibrated GC using mesitylene as the internal standard. 4-Bromostyrene was used as the analyte. [d] ^{1}H NMR yield of **3a**. [e] Irradiated for 90 min.

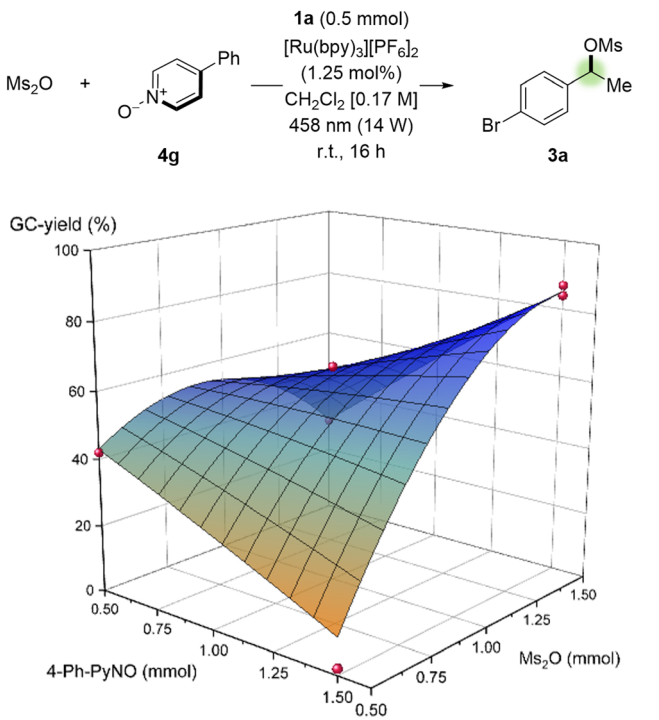

Fig. 2 Simulated 3D surface plot of the DoE-assisted optimization of the reagent ratios. 1-Bromo-4-ethylbenzene (**1a**, 0.5 mmol) was used as the limiting reagent. Yields were determined by calibrated GC. 4-Bromostyrene was used as the analyte.

conditions for this experiment comprised the use of the substrate **1a** as the limiting reagent, in conjunction with both reagents *N*-oxide **4g** and methanesulfonic anhydride, in equimolar amounts and threefold excess. In total, the energy consumption of the reaction set-up accounted for 24 Wh.[55]

With the optimized reaction conditions in hand, our next objective was to investigate the applicability of the established protocol. As demonstrated by Fritz-Langhals as well as Ritter and colleagues, the isolation of the corresponding benzylic mesylate or its *in situ* conversion under standardized reaction conditions poses a challenge.[49,56] Driven by our interest in the synthesis of drug metabolites, we consequently concentrated on the synthesis of benzylic alcohols by nucleophilic substitution of the benzylic mesylates **3** (Scheme 3).

A considerable variety of mesylates **3a–3y** were successfully transformed into the targeted benzyl alcohols **5a–5y** under both basic and acidic conditions. To ensure the reproducibility of the reaction procedure, all scope entries were run in two separate experiments and the isolated yields are shown as average yields within a standard deviation of ≤5%. We first tested a variety of ethyl arenes (Scheme 3, top). Several ethyl arenes bearing (pseudo)halide substituents as well as unsubstituted ethylbenzene were converted into the corresponding 1-phenethyl alcohols **5a–5g** in isolated yields of 52–71%. The

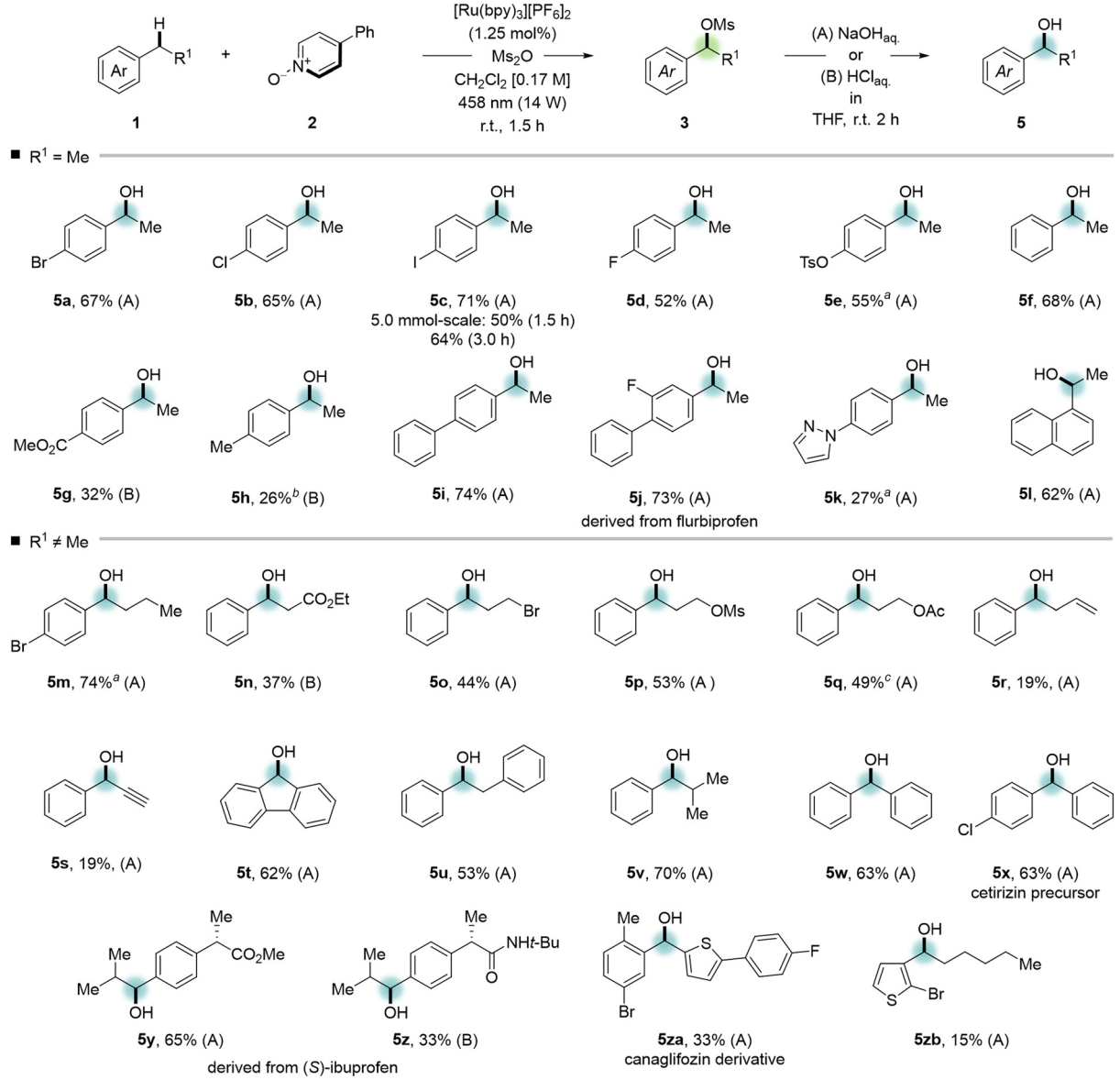

Scheme 3 Reaction scope of the benzylic C–H bond oxygenation. Reactions were run on a 0.5 mmol scale, using **1** (1.0 equiv.), 4-phenylpyridine *N*-oxide (**4g**) (3.0 equiv.), Ms_2O (3.0 equiv.) and $[Ru(bpy)_3][PF_6]_2$ (1.25 mol%) in CH_2Cl_2 [0.17 M]. Irradiation with two LED panels (458 nm, 2 × 7 W). Yields refer to isolated material over two steps and are listed as the average of two experiments within a standard deviation of 5%. [a] Irradiated for 2.5 h. [b] Irradiated for 0.5 h. [c] Hydrolysis for 0.5 h.

10-fold scale-up of the photo-mediated benzylic oxygenation was successfully realized using 1-iodo-4-ethylbenzene (**1c**). The corresponding benzylic alcohol **5c** was obtained in 64% isolated yield over two steps after a prolonged irradiation time of 3 h. Polycyclic benzyl alcohols **5i**, the flurbiprofen derivative **5j**, and **5l** were obtained in good yields of up to 75%. 1-Ethyl-4-methylbenzene (**5h**) bearing two competing benzylic positions for C–H bond scission was converted into the secondary benzylic alcohol **5h** in 26% yield after 0.5 h.[57] Notably, although benzylic mesylates are sensitive to elimination at temperatures above 60 °C, methane sulfonate hydrolysis and nucleophilic substitution with sodium hydroxide predominates over E2 elimination. Notably, when treating the benzylic mesylate with primary amines, sulfonate hydrolysis to the corresponding benzylic alcohol was observed exclusively. The mesylates of esters **1g** and **1n**, containing base-sensitive functional groups, were converted under acidic conditions using HCl (1.0 M) in THF : H_2O. Next, we examined substrates bearing diverse sidechains (Scheme 3, bottom). 1-(4-Bromophenyl)butan-1-ol (**5m**) was isolated in 74% yield after a prolonged reaction time of 2.5 h. Substrates bearing various functional groups on the alkyl chain such as esters, halides, and mesylates were readily converted into the corresponding alcohol derivatives **5n**, **5o**, **5p** and **5q** in good yields. Alkenyl and alkyne substitution resulted in a decreased yield of 19%. 9*H*-Fluoren-9-ol (**5t**) was isolated in 62% yield. Steric bulk at the α-position to the benzylic C–H bond as evident in products **5u**, **5v**, **5y** and **5z** did not impair the product yields. Significantly, methyl (*S*)-ibuprofen underwent selective oxidation on the isobutyl sidechain to produce alcohol **5y**, effectively leaving the more acidic propanoate C–H bond intact. The (*S*),(*R*)- and (*S*),(*S*)-diastereomers of **5y** were formed in equimolar quantities.

In contrast, sterically encumbered phthalimide-protected phenylalanine **1x** allowed isolation of the benzylic mesylate **3x** as a mixture of diastereomers in a ratio of 86 : 14 (Scheme 4, top). The major product obtained, exhibited high crystallinity suitable for X-ray spectroscopic analysis and the major diastereomer was unequivocally identified as the (2*S*,3*S*) stereoisomer. Notably, nucleophilic substitution was most effective under the conditions described by Ritter and co-workers, utilizing HFIP and water, which resulted in the conversion into the (2*S*,3*R*)-3-hydroxyphenylalanine derivative **5x** as a single isomer upon inversion of the stereogenic centre, based on spectroscopic and crystallographic analysis (Scheme 4, top).[49,58] The synthetic utility is demonstrated by the practical synthesis of diphenhydramine (**10**), a first generation H_1-antihistamine, from diphenylmethane (**1w**) without intermediate

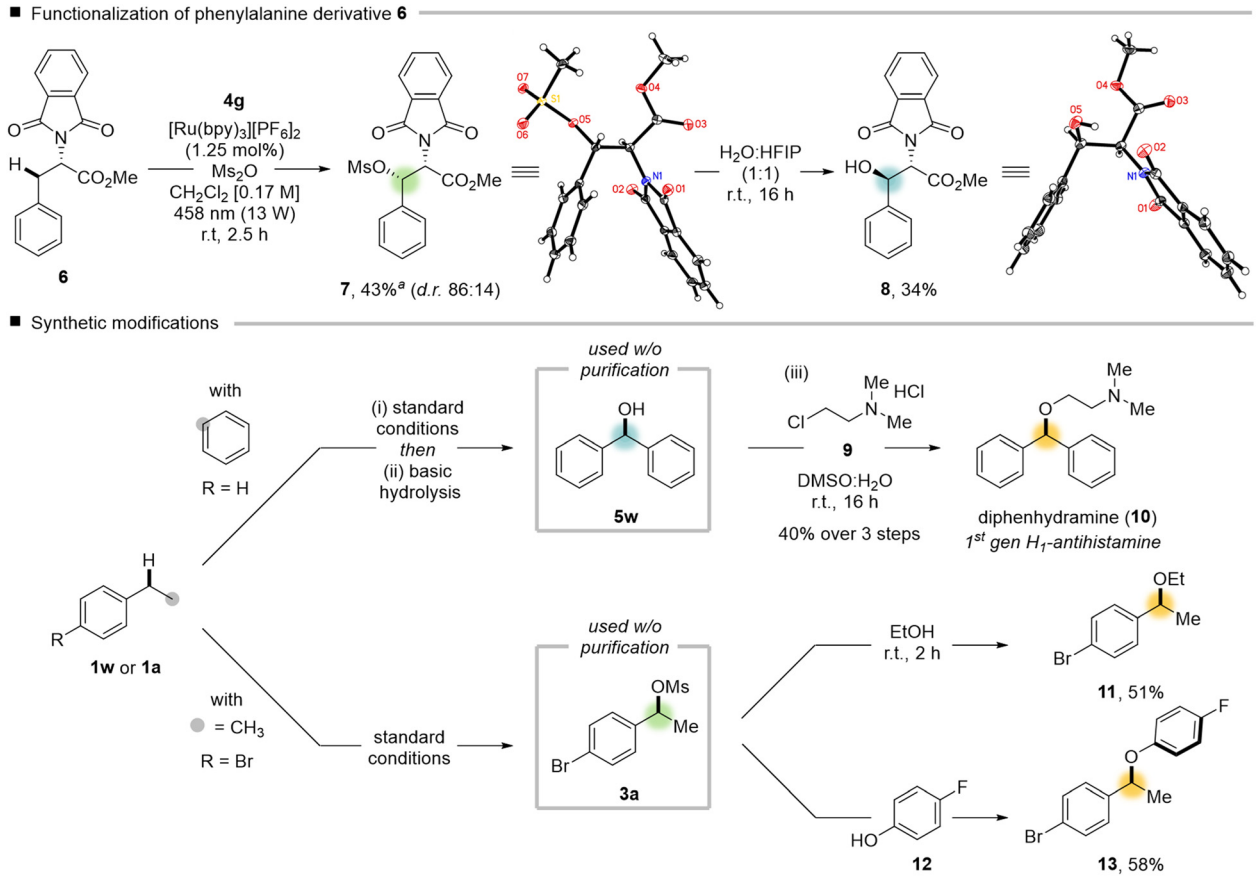

Scheme 4 Benzylic C–H bond functionalization of phenylalanine derivative **6** and synthetic derivatization.

purification in 40% overall yield. In addition, benzylic mesylates can be utilised as electrophiles in nucleophilic substitution reactions, employing ethanol or 4-fluorophenol (**12**) (Scheme 4, bottom).[59]

Next, we focused on investigating the underlying mechanistic aspects of the benzylic C–H bond mesyloxylation strategy. The corroborated mechanism is depicted in Fig. 3. Stern–Volmer quenching experiments confirmed that 1-(methylsulfonyloxy)pyridinium methanesulfonate (**2**) was identified as the most effective quencher of the excited catalyst (K_{SV} = 54.8 M^{-1}). With a ground state reduction potential of $E^{red}_{1/2} = -0.42$ V for **2** and $E^{red}_{1/2} = -0.46$ V for **2g** in MeCN *vs.* SCE, a single electron reduction by the excited state photoredox catalyst [Ru(bpy)$_3$][PF$_6$]$_2$ ($E^{*}_{ox} = -0.81$ V *vs.* SCE in MeCN, λ^{abs}_{max} = 450 nm)[52] is feasible. The single-electron reduction populates the π*-orbital of the heteroarene. A concomitant out-of-plane bending of the exocyclic σ-bond leads to the population of the σ*-orbital due to canonical intersection.[17] As a result, the bond weakens, ultimately causing N–O bond scission. Homolytic bond cleavage of the exocyclic N–O bond leads to the generation of 4-phenylpyridine (**6**) and the methylsulfonyloxy radical **MsO**$^{\bullet}$. Alkylsulfonyloxy radicals (BDE = 107 kcal mol^{-1} for BuSO$_3$H) are apt to cleave benzylic C–H bonds (BDE = 88 kcal mol^{-1} for 4-bromoethylbenzene) through HAT forming a benzylic C-centered radical **1**$^{\bullet}$.[60,61] The resulting methanesulfonic acid is captured by 4-phenylpyridine (**6**) forming a weakly acidic acid–base adduct. The oxidation of the stabilized benzylic radical (**1**$^{+}$, $E^{ox}_{1/2}$ = +0.73 V for PhCH$_2^{\bullet}$ and +0.37 V for PhC$^{\bullet}$HCH$_3$ *vs.* SCE in MeCN)[62] by the oxidized form of the photoredox catalyst ($E^{ox}_{1/2}$[Ru^{III}/Ru^{II}] = +1.29 V *vs.* SCE)[52] closes the catalytic cycle. Subsequently, the resulting benzylic carbocation reacts with a methanesulfonate anion to form 1-phenylalkyl methanesulfonates **3** as the final product, in line with an ORPC mechanism.

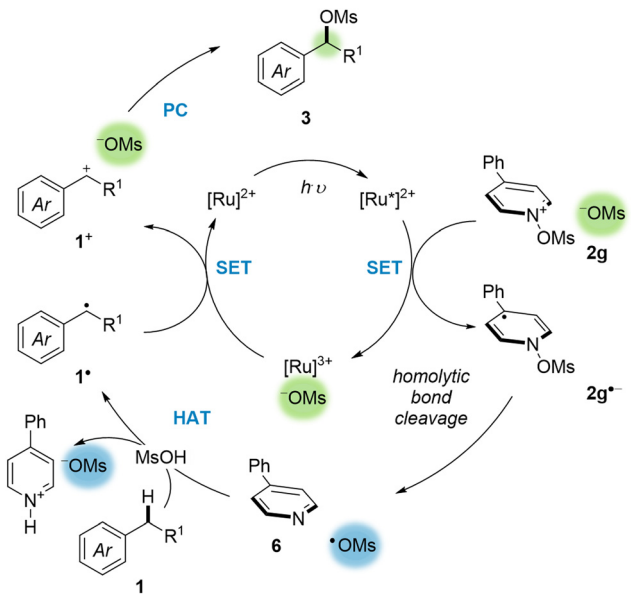

Fig. 3 Proposed catalytic cycle.

The kinetic isotope effect (KIE) of the benzylic C–H bond cleavage was determined by an intramolecular competition experiment (Scheme 5, top). 4-(Ethyl-1-*d*)-2-fluoro-1,1′-biphenyl (***d*-1j**) with 90% deuterium content was prepared by photomediated deuterodecarboxylation of flurbiprofen and subjected to the standard reaction conditions.[63] The analysis of the crude NMR spectra towards the synthesis of alcohol ***d*-5j** revealed a significant kinetic isotope effect of 3.85. When 4-phenylbutanoic acid (**14**) was used as the substrate, 5-phenyldihydrofuran-2(3*H*)-one (**15**) was isolated as a single product in 39% yield (Scheme 5, bottom). The cyclization suggests the presence of a benzylic carbocation intermediate.

To better understand the divergent behaviour between (methylsulfonyloxy)pyridinium salts and their trifluoromethylsulfonyloxy counterparts, we conducted density functional theory (DFT) calculations. Geometry optimization and frequency calculations were performed using the B3LYP/6-31G(d) level of theory using Gaussian 16 software.[64] To provide further insights into the electronic structures, natural bond orbital (NBO) analyses were conducted utilizing NBO 6.0 software.[65] The optimized structures reveal the out-of-plane bending of the exocyclic N–O bond, which is crucial for the population of the (N–O) σ*-orbital for bond cleavage.[66–68] The NBO analysis of the pyridinium moieties **pyOMs**$^{\bullet}$ and **pyOTf**$^{\bullet}$ post-single electron reduction can be represented as a two-centre-three-electron (2c–3e) bond scenario (Fig. 4A illustrates this for **pyOMs**$^{\bullet}$). To model bond cleavage during the DET process, both homolytic and heterolytic bond scissions were simulated. The solvation effects were accounted for using the solvation model based on density (SMD) as implemented in Gaussian 16.[70] The solvent used for the SMD calculations was dichloromethane (ε = 8.93), chosen to mimic the experimental conditions. The bond dissociation energy of **pyOTf**$^{\bullet}$ is found to be barrierless and exergonic, with a release of approximately 3.0 kcal mol^{-1} in both cases (Fig. 4, left). Experimental validation of the reactivity of the corresponding pyridyl radical

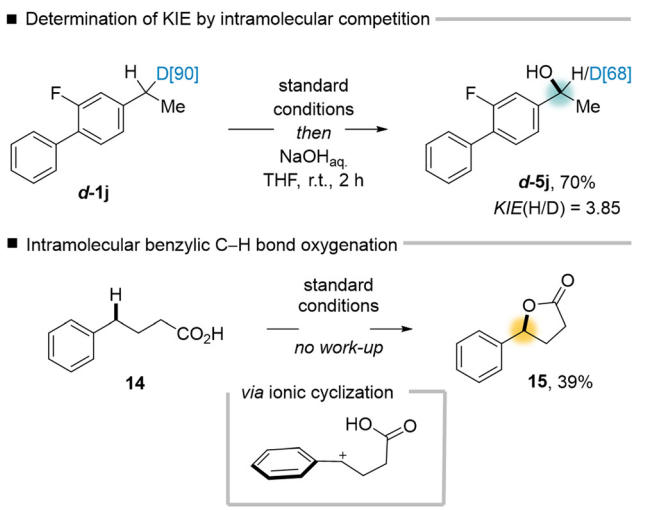

Scheme 5 Determination of the KIE (top); intramolecular benzylic C–H bond oxygenation (bottom).

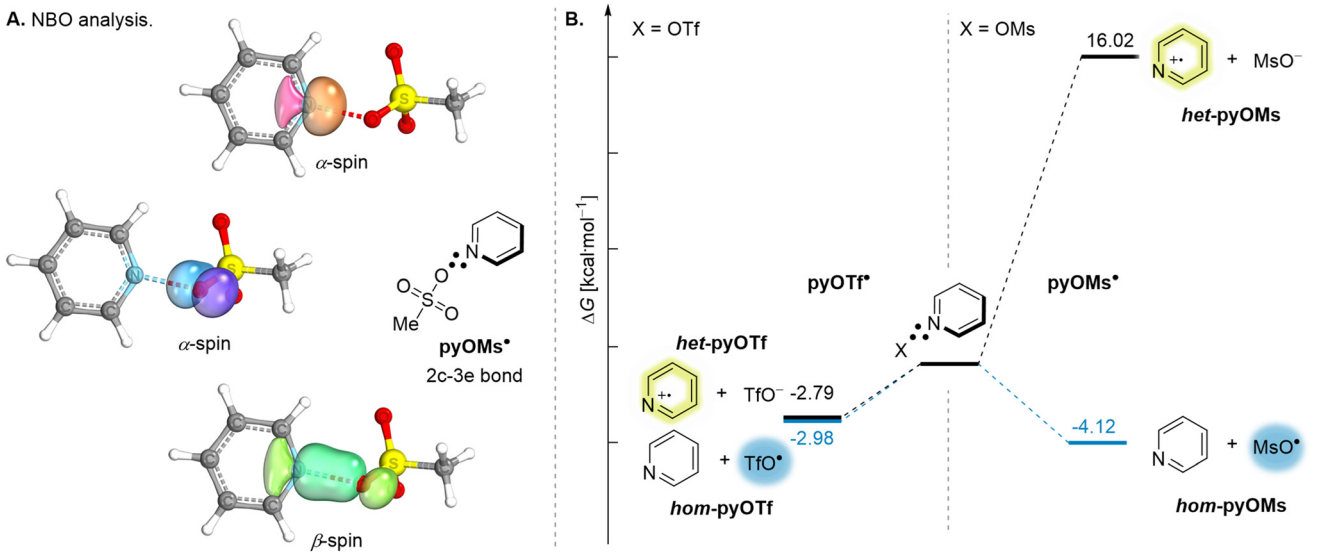

Fig. 4 (A) Depiction of the relevant orbitals associated with the 2c–3e bond scenario in **pyOMs**•. Orbitals were visualized using **Iboview**, Version v20211019-RevA (G. Knizia, Available at: https://www.iboview.org).[69] (B) Relative reaction coordinate profile for the homolytic and heterolytic N–O bond cleavage of **pyOTf**• and **pyOMs**•, respectively.

during heterolytic bond cleavage was provided by Togni, Carreira and Ritter.[18–21] Conversely, the O-centered triflyloxy radical is deemed unstable and thus prone to dissociation.[33] In contrast, the heterolytic N–O bond cleavage of **pyOMs**• was computationally determined to be endergonic by +16.0 kcal mol^{-1}. In contrast, the homolytic cleavage, resulting in the formation of a stable O-centered mesyloxy radical, is exergonic by −4.1 kcal mol^{-1} (Fig. 4B, right). Hence, the applied model reflects the observed reaction outcome described in this account. Both experimental and theoretical analyses underscore the significance of electronic effects on radical generation.[16]

In summary, we have established a straightforward and scalable procedure for the radical mesyloxylation of benzylic C–H bonds. The mesyloxy radical originates from the homolytic cleavage of an *in situ* generated pyridinium salt. This *in situ* formation of pyridinium salts from heteroarene *N*-oxides and methanesulfonic anhydride enabled efficient screening of redox-active functional group transfer reagents. The selective mesyloxylation of benzylic C–H bonds enables the targeted synthesis of benzyl mesylates, which can then be either directly derivatized or converted into the corresponding alcohols using a simple and unified approach. The developed methodology is distinguished by its operational simplicity, rapid reaction at low wattage, and minimal energy consumption for the functionalization of a wide range of substrates.

Author contributions

TT, JS, and XS performed the optimization of the reaction conditions. JT, XS and JS elaborated on the scope of the reaction. TT and JT conducted mechanistic experiments. TT performed the DFT calculations. JP conceived the idea and guided the progress of this work. The manuscript was written through contributions from JP, TT, and JT. All authors have approved the final version of the manuscript.

Conflicts of interest

The authors declare no competing financial interests.

Abbreviations

HAT	Hydrogen atom transfer
ORPC	Oxidative radical polar crossover
DET	Dissociative electron transfer
SET	Single electron transfer
KIE	Kinetic isotope effect
HFIP	Hexafluoro isopropanol

Data availability

All experimental data supporting the findings of this study are available within the article and its ESI.† Crystallographic data for the structures reported in this work have been deposited with the Cambridge Crystallographic Data Centre under deposition numbers CCDC (2345289 and 2348388†). Structural parameters (Cartesian coordinates) for all DFT-optimized structures are provided as a separate dataset alongside the ESI.† Additional raw data, spectral files, and analysis scripts are available from the corresponding author upon reasonable request.

Acknowledgements

We extend our gratitude to Ludwig Lorenzen for synthesizing the starting material 1k. J. T. gratefully acknowledges the financial support from the Studienstiftung des Deutschen Volkes in the form of a doctoral scholarship. The work was supported by the German Research Foundation (DFG, 401007518). We thank the technical and analytical staff at LIKAT for their assistance. Special thanks go to Dr Anke Spannenberg and Dr Hans-Joachim Drexler for X-ray crystallographic analysis and to Dr Fabian Reiß for his assistance with DFT calculations. Dr Dirk Michalik and Jonas Bresien are acknowledged for their assistance with specialized NMR measurements related to this study and Prof. Torsten Beweries for fruitful discussions.

References

1 T. Cernak, K. D. Dykstra, S. Tyagarajan, P. Vachal and S. W. Krska, The medicinal chemist's toolbox for late stage functionalization of drug-like molecules, *Chem. Soc. Rev.*, 2016, **45**, 546–576.
2 R. de Jesus, K. Hiesinger and M. van Gemmeren, Preparative Scale Applications of C–H Activation in Medicinal Chemistry, *Angew. Chem., Int. Ed.*, 2023, **62**, e202306659.
3 J. C. K. Chu and T. Rovis, Complementary Strategies for Directed C(sp3)–H Functionalization: A Comparison of Transition-Metal-Catalyzed Activation, Hydrogen Atom Transfer, and Carbene/Nitrene Transfer, *Angew. Chem., Int. Ed.*, 2018, **57**, 62–101.
4 T. Gensch, M. N. Hopkinson, F. Glorius and J. Wencel-Delord, Mild metal-catalyzed C–H activation: examples and concepts, *Chem. Soc. Rev.*, 2016, **45**, 2900–2936.
5 C. Ma, P. Fang and T.-S. Mei, Recent Advances in C–H Functionalization Using Electrochemical Transition Metal Catalysis, *ACS Catal.*, 2018, **8**, 7179–7189.
6 S. Sarkar, K. P. S. Cheung and V. Gevorgyan, C–H functionalization reactions enabled by hydrogen atom transfer to carbon-centered radicals, *Chem*, 2020, **11**, 12974–12993.
7 L. Guillemard, N. Kaplaneris, L. Ackermann and M. J. Johansson, Late-stage C–H functionalization offers new opportunities in drug discovery, *Nat. Rev. Chem.*, 2021, **5**, 522–545.
8 N. Holmberg-Douglas and D. A. Nicewicz, Photoredox-Catalyzed C–H Functionalization Reactions, *Chem. Rev.*, 2022, **122**, 1925–2016.
9 R. J. Wiles and G. A. Molander, Photoredox-Mediated Net-Neutral Radical/Polar Crossover Reactions, *Isr. J. Chem.*, 2020, **60**, 281–293.
10 D. Wang, L. Désaubry, G. Li, M. Huang and S. Zheng, Front Cover Picture: Recent Advances in the Synthesis of C2-Functionalized Pyridines and Quinolines Using N-Oxide Chemistry (Adv. Synth. Catal. 1/2021), *Adv. Synth. Catal.*, 2021, **363**, 1–1.
11 J. Boström, D. G. Brown, R. J. Young and G. M. Keserü, Expanding the medicinal chemistry synthetic toolbox, *Nat. Rev. Drug Discovery*, 2018, **17**, 709–727.
12 C. R. Zwick III and H. Renata, Remote C–H Hydroxylation by an α-Ketoglutarate-Dependent Dioxygenase Enables Efficient Chemoenzymatic Synthesis of Manzacidin C and Proline Analogs, *J. Am. Chem. Soc.*, 2018, **140**, 1165–1169.
13 F. Xue, H. Lu, L. He, W. Li, D. Zhang, X.-Y. Liu and Y. Qin, Formal Total Syntheses of (−)- and (+)-Actinophyllic Acid, *J. Org. Chem.*, 2018, **83**, 754–764.
14 R. Cannalire, S. Pelliccia, L. Sancineto, E. Novellino, G. C. Tron and M. Giustiniano, Visible light photocatalysis in the late-stage functionalization of pharmaceutically relevant compounds, *Chem. Soc. Rev.*, 2021, **50**, 766–897.
15 P. Bellotti, H.-M. Huang, T. Faber and F. Glorius, Photocatalytic Late-Stage C–H Functionalization, *Chem. Rev.*, 2023, **123**, 4237–4352.
16 A. Ruffoni, R. C. Mykura, M. Bietti and D. Leonori, The interplay of polar effects in controlling the selectivity of radical reactions, *Nat. Synth.*, 2022, **1**, 682–695.
17 E. D. Lorance, W. H. Kramer and I. R. Gould, Kinetics of Reductive N–O Bond Fragmentation: The Role of a Conical Intersection, *J. Am. Chem. Soc.*, 2002, **124**, 15225–15238.
18 S. L. Rössler, B. J. Jelier, E. Magnier, G. Dagousset, E. M. Carreira and A. Togni, Pyridinium Salts as Redox-Active Functional Group Transfer Reagents, *Angew. Chem., Int. Ed.*, 2020, **59**, 9264–9280.
19 T. W. Greulich, C. G. Daniliuc and A. Studer, N-Aminopyridinium Salts as Precursors for N-Centered Radicals – Direct Amidation of Arenes and Heteroarenes, *Org. Lett.*, 2015, **17**, 254–257.
20 W. S. Ham, J. Hillenbrand, J. Jacq, C. Genicot and T. Ritter, Divergent Late-Stage (Hetero)aryl C–H Amination by the Pyridinium Radical Cation, *Angew. Chem., Int. Ed.*, 2019, **58**, 532–536.
21 S. L. Rössler, B. J. Jelier, P. F. Tripet, A. Shemet, G. Jeschke, A. Togni and E. M. Carreira, Pyridyl Radical Cation for C–H Amination of Arenes, *Angew. Chem., Int. Ed.*, 2019, **58**, 526–531.
22 B. J. Jelier, P. F. Tripet, E. Pietrasiak, I. Franzoni, G. Jeschke and A. Togni, Radical Trifluoromethoxylation of Arenes Triggered by a Visible-Light-Mediated N–O Bond Redox Fragmentation, *Angew. Chem., Int. Ed.*, 2018, **57**, 13784–13789.
23 K. Miyazawa, T. Koike and M. Akita, Regiospecific Intermolecular Aminohydroxylation of Olefins by Photoredox Catalysis, *Chem. – Eur. J.*, 2015, **21**, 11677–11680.
24 K. Miyazawa, T. Koike and M. Akita, Aminohydroxylation of olefins with iminopyridinium ylides by dual Ir photocatalysis and $Sc(OTf)_3$ catalysis, *Tetrahedron*, 2016, **72**, 7813–7820.
25 F. J. R. Klauck, M. J. James and F. Glorius, Deaminative Strategy for the Visible-Light-Mediated Generation of Alkyl Radicals, *Angew. Chem., Int. Ed.*, 2017, **56**, 12336–12339.

26 S.-Z. Sun, C. Romano and R. Martin, Site-Selective Catalytic Deaminative Alkylation of Unactivated Olefins, *J. Am. Chem. Soc.*, 2019, **141**, 16197–16201.
27 Z.-F. Zhu, J.-L. Tu and F. Liu, Ni-Catalyzed deaminative hydroalkylation of internal alkynes, *Chem. Commun.*, 2019, **55**, 11478–11481.
28 J. Wu, P. S. Grant, X. Li, A. Noble and V. K. Aggarwal, Catalyst-Free Deaminative Functionalizations of Primary Amines by Photoinduced Single-Electron Transfer, *Angew. Chem., Int. Ed.*, 2019, **58**, 5697–5701.
29 J. W. Beatty, J. J. Douglas, K. P. Cole and C. R. J. Stephenson, A scalable and operationally simple radical trifluoromethylation, *Nat. Commun.*, 2015, **6**, 7919.
30 J. W. Beatty, J. J. Douglas, R. Miller, R. C. McAtee, K. P. Cole and C. R. J. Stephenson, Photochemical Perfluoroalkylation with Pyridine N-Oxides: Mechanistic Insights and Performance on a Kilogram Scale, *Chem*, 2016, **1**, 456–472.
31 Y. Ouyang, X.-H. Xu and F.-L. Qing, Trifluoromethanesulfonic Anhydride as a Low-Cost and Versatile Trifluoromethylation Reagent, *Angew. Chem., Int. Ed.*, 2018, **57**, 6926–6929.
32 T. Tsuruta, D. Spinnato, H. W. Moon, M. Leutzsch and J. Cornella, Bi-Catalyzed Trifluoromethylation of C(sp2)–H Bonds under Light, *J. Am. Chem. Soc.*, 2023, **145**, 25538–25544.
33 R. E. Noftle and G. H. Cady, Preparation and Properties of Bis(trifluoromethylsulfuryl) Peroxide and Trifluoromethyl Trifluoromethanesulfonate, *Inorg. Chem.*, 1965, **4**, 1010–1012.
34 L. Capaldo and D. Ravelli, Hydrogen Atom Transfer (HAT): A Versatile Strategy for Substrate Activation in Photocatalyzed Organic Synthesis, *Eur. J. Org. Chem.*, 2017, 2056–2071.
35 L. Capaldo, L. L. Quadri and D. Ravelli, Photocatalytic hydrogen atom transfer: the philosopher's stone for late-stage functionalization?, *Green Chem.*, 2020, **22**, 3376–3396.
36 G.-X. Li, C. A. Morales-Rivera, F. Gao, Y. Wang, G. He, P. Liu and G. Chen, A unified photoredox-catalysis strategy for C(sp3)–H hydroxylation and amidation using hypervalent iodine, *Chem*, 2017, **8**, 7180–7185.
37 J. M. Paolillo, A. D. Duke, E. S. Gogarnoiu, D. E. Wise and M. Parasram, Anaerobic Hydroxylation of C(sp3)–H Bonds Enabled by the Synergistic Nature of Photoexcited Nitroarenes, *J. Am. Chem. Soc.*, 2023, **145**, 2794–2799.
38 B. J. Lee, K. S. DeGlopper and T. P. Yoon, Site-Selective Alkoxylation of Benzylic C–H Bonds by Photoredox Catalysis, *Angew. Chem., Int. Ed.*, 2020, **59**, 197–202.
39 C. Bo, F. Chen, Q. Bu, Z.-H. Du, M. Li, B. Dai and N. Liu, Visible-Light-Driven Organocatalytic Alkoxylation of Benzylic C–H Bonds, *J. Org. Chem.*, 2023, **88**, 3532–3538.
40 K. Yamashita, F. Kawahara and Y. Hamashima, Benzylic C(sp3)–H Alkoxylation through Visible-Light-Driven Oxidative Radical-Polar Crossover, *Asian J. Org. Chem.*, 2024, **13**, e202300662.
41 Y. Zhang, P. K. Sahoo, P. Ren, Y. Qin, R. Cauwenbergh, P. Nimmegeers, G. SivaRaman, S. Van Passel, A. Guidetti and S. Das, Transition metal-free approach for late-stage benzylic C(sp3)–H etherifications and esterifications, *Chem. Commun.*, 2022, **58**, 11454–11457.
42 N. A. Fitzpatrick, L. Zamani, M. Das, H. G. Yayla, M. S. Lall and P. Z. Musacchio, A SN1 mechanistic approach to the Williamson ether reaction via photoredox catalysis applied to benzylic C(sp3)–H bonds, *Tetrahedron*, 2022, **125**, 132986.
43 M. Dong, Y. Jia, W. Zhou, J. Gao, X. Lv, F. Luo, Y. Zhang and S. Liu, A photoredox/nickel dual-catalytic strategy for benzylic C–H alkoxylation, *Org. Chem. Front.*, 2021, **8**, 6881–6887.
44 D. L. Golden, C. Zhang, S.-J. Chen, A. Vasilopoulos, I. A. Guzei and S. S. Stahl, Benzylic C–H Esterification with Limiting C–H Substrate Enabled by Photochemical Redox Buffering of the Cu Catalyst, *J. Am. Chem. Soc.*, 2023, **145**, 9434–9440.
45 M. E. Ruos, R. G. Kinney, O. T. Ring and A. G. Doyle, A General Photocatalytic Strategy for Nucleophilic Amination of Primary and Secondary Benzylic C–H Bonds, *J. Am. Chem. Soc.*, 2023, **145**, 18487–18496.
46 I. N.-M. Leibler, M. A. Tekle-Smith and A. G. Doyle, A general strategy for C(sp3)–H functionalization with nucleophiles using methyl radical as a hydrogen atom abstractor, *Nat. Commun.*, 2021, **12**, 6950.
47 Y. Zhang, N. A. Fitzpatrick, M. Das, I. P. Bedre, H. G. Yayla, M. S. Lall and P. Z. Musacchio, A photoredox-catalyzed approach for formal hydride abstraction to enable C-H functionalization with nucleophilic partners (F, C, O, N, and Br/Cl), *Chem. Catal.*, 2022, **2**, 292–308.
48 M. Das, L. Zamani, C. Bratcher and P. Z. Musacchio, Azolation of Benzylic C–H Bonds via Photoredox-Catalyzed Carbocation Generation, *J. Am. Chem. Soc.*, 2023, **145**, 3861–3868.
49 L. Tanwar, J. Börgel and T. Ritter, Synthesis of Benzylic Alcohols by C–H Oxidation, *J. Am. Chem. Soc.*, 2019, **141**, 17983–17988.
50 J. Börgel, L. Tanwar, F. Berger and T. Ritter, Late-Stage Aromatic C–H Oxygenation, *J. Am. Chem. Soc.*, 2018, **140**, 16026–16031.
51 T. Taeufer, A. Spannenberg and J. Pospech, 1-[(Methylsulfonyl)oxy]pyridin-1-ium methanesulfonate, *IUCrData*, 2021, **6**, x211026.
52 C. K. Prier, D. A. Rankic and D. W. C. MacMillan, Visible Light Photoredox Catalysis with Transition Metal Complexes: Applications in Organic Synthesis, *Chem. Rev.*, 2013, **113**, 5322–5363.
53 Benzylic mesylates undergo elimination to styrenes under GC conditions, inflating GC yields. ^{1}H NMR yields, determined after solvent removal at ambient temperature, more accurately reflect the actual product yield. (see ESI, page S16†).
54 R. Leardi, Experimental design in chemistry: A tutorial, *Anal. Chim. Acta*, 2009, **652**, 161–172.
55 For detailed information, see ESI page S11.†
56 E. Fritz-Langhals, Synthesis of optically active 1-fluoroalkyl benzenes, *Tetrahedron Lett.*, 1994, **35**, 1851–1854.

57 The mesyloxyation step proceeded in 42% yield according to NMR. Longer reaction times resulted in product mixtures.
58 Deposition numbers 2345289 (for **7**) and 2348388 (for **8**)† contain the supplementary crystallographic data for this paper. These data are provided free of charge by the joint Cambridge Crystallographic Data Centre and Fachinformationszentrum Karlsruhe Access Structures service.
59 Substrates bearing multiple reactive C–H sites, particularly α to basic amines, showed limited reactivity under current conditions; further development is underway to address these challenges (see ESI, page S57†).
60 Y.-R. Luo, *Comprehensive handbook of chemical bond energies*, CRC Press, Boca Raton, FL, 2007.
61 M. Griesser, J.-P. R. Chauvin and D. A. Pratt, The hydrogen atom transfer reactivity of sulfinic acids, *Chem*, 2018, **9**, 7218–7229.
62 D. D. M. Wayner, D. J. McPhee and D. Griller, *J. Am. Chem. Soc.*, 1988, **110**, 132–137.
63 T. S. Mayer, T. Taeufer, S. Brandt, J. Rabeah and J. Pospech, Photomediated Hydro- and Deuterodecarboxylation of Pharmaceutically Relevant and Natural Aliphatic Carboxylic Acids, *J. Org. Chem.*, 2023, **88**, 6347–6353.
64 M. J. Frisch, G. W. Trucks, H. B. Schlegel, G. E. Scuseria, M. A. Robb, J. R. Cheeseman, G. Scalmani, V. Barone, G. A. Petersson, H. Nakatsuji, X. Li, M. Caricato, A. V. Marenich, J. Bloino, B. G. Janesko, R. Gomperts, B. Mennucci, H. P. Hratchian, J. V. Ortiz, A. F. Izmaylov, J. L. Sonnenberg, D. Williams-Young, F. Ding, F. Lipparini, F. Egidi, J. Goings, B. Peng, A. Petrone, T. Henderson, D. Ranasinghe, V. G. Zakrzewski, J. Gao, N. Rega, G. Zheng, W. Liang, M. Hada, M. Ehara, K. Toyota, R. Fukuda, J. Hasegawa, M. Ishida, T. Nakajima, Y. Honda, O. Kitao, H. Nakai, T. Vreven, K. Throssell, J. A. Montgomery Jr., J. E. Peralta, F. Ogliaro, M. J. Bearpark, J. J. Heyd, E. N. Brothers, K. N. Kudin, V. N. Staroverov, T. A. Keith, R. Kobayashi, J. Normand, K. Raghavachari, A. P. Rendell, J. C. Burant, S. S. Iyengar, J. Tomasi, M. Cossi, J. M. Millam, M. Klene, C. Adamo, R. Cammi, J. W. Ochterski, R. L. Martin, K. Morokuma, O. Farkas, J. B. Foresman and D. J. Fox, Gaussian 16, Revision C.01, Gaussian, Inc., Wallingford CT, 2016.
65 E. Glendening, J. Badenhoop, A. Reed, J. Carpenter, J. Bohmann, C. Morales, C. Landis and F. Weinhold, *NBO 6.0*, Theoretical Chemistry Institute, University of Wisconsin, Madison, WI, 2013, p. 2011.
66 E. D. Lorance, K. Hendrickson and I. R. Gould, Density Functional Theory Predicts the Barriers for Radical Fragmentation in Solution, *J. Org. Chem.*, 2005, **70**, 2014–2020.
67 D. Laage, I. Burghardt, T. Sommerfeld and J. T. Hynes, On the Dissociation of Aromatic Radical Anions in Solution. 1. Formulation and Application to p-Cyanochlorobenzene Radical Anion, *J. Phys. Chem. A*, 2003, **107**, 11271–11291.
68 E. D. Lorance and I. R. Gould, A Quantitative Curve-Crossing Model for Radical Fragmentation, *J. Phys. Chem. A*, 2005, **109**, 2912–2919.
69 G. Knizia, Intrinsic Atomic Orbitals: An Unbiased Bridge between Quantum Theory and Chemical Concepts, *J. Chem. Theory Comput.*, 2013, **9**, 4834–4843.
70 A. V. Marenich, C. J. Cramer and D. G. Truhlar, Universal Solvation Model Based on Solute Electron Density and on a Continuum Model of the Solvent Defined by the Bulk Dielectric Constant and Atomic Surface Tensions, *J. Phys. Chem. B*, 2009, **113**, 6378–6396.

